Catalysis Letters 30 (1995) 53–63

Incorporation of La^{3+} into a $Pt/CeO_2/Al_2O_3$ catalyst

R.K. Usmen, G.W. Graham, W.L.H. Watkins and R.W. McCabe

Ford Motor Company, Ford Research Laboratory, PO Box 2053, MD 3179, Dearborn, MI 48121-2053, USA

Received 1 August 1994; accepted 14 September 1994

The effects of La^{3+} incorporation into a $Pt/CeO_2/Al_2O_3$ catalyst were investigated by a combination of activity, temperature-programmed reduction (TPR), oxygen storage capacity (OSC), noble-metal surface area, and X-ray diffraction (XRD) measurements. Incorporation of La^{3+} ions into the Al_2O_3, before CeO_2 is added, promoted higher Pt and CeO_2 dispersions. The oxygen storage capacity was also higher in the presence of La^{3+}. This is attributed to a combination of Pt and CeO_2 particle-size effects and possible blockage of the reaction between Al_2O_3 and CeO_2. The XRD data show that La^{3+} forms $LaAlO_3$ with Al_2O_3 and prevents α-Al_2O_3 formation after various heat treatments.

Keywords: lanthana; alumina; ceria; Pt; three-way catalyst; oxygen storage; X-ray diffraction; CO chemisorption; temperature-programmed reduction

1. Introduction

The present-day automotive three-way catalyst (TWC) contains a number of ingredients, each typically intended to perform a particular function. Lanthana (La_2O_3), for example, known to be one of the most effective inhibitors of alumina surface area loss [1], has long been added at levels required to optimally achieve just this result. But the addition of La_2O_3 has also been linked to other effects such as increased rich-side NO_x conversion in Pd-based catalysts [2] and higher noble-metal dispersion [3]. Recent observations [4] suggest that La_2O_3 may further promote more efficient utilization of yet another ingredient of the TWC, ceria (CeO_2), which serves primarily as an oxygen storage component [5–12]. Specifically, La^{3+}-modified alumina-supported ceria was found to display a smaller intrinsic Ce^{3+} fraction, a larger CeO_2 dispersion, and a greater range of reversible reducibility than in the unmodified case. The present study, incorporating Pt as a catalytically active ingredient, was undertaken to determine whether these changes translate into observable effects in an actual catalyst.

2. Experimental

2.1. CATALYST PREPARATION

Samples of 10 wt% La_2O_3/γ-Al_2O_3 and 10 wt% CeO_2/γ-Al_2O_3 catalysts were prepared by impregnating γ-Al_2O_3 washcoated ceramic cordierite with $La(NO_3)_3 \cdot 5H_2O$ and $Ce(NO_3)_3 \cdot 6H_2O$ solutions of the desired concentration by the incipient wetness method. The samples were dried at 373 K and calcined at 773 K for 5 h. The 10 wt% CeO_2/10 wt% La_2O_3/γ-Al_2O_3 sample was prepared by impregnating the calcined 10 wt% La_2O_3/γ-Al_2O_3 sample with $Ce(NO_3)_3 \cdot 6H_2O$ solution of the desired concentration. This sample was again dried at 373 K and calcined at 773 K for 5 h.

Catalysts containing 0.6 wt% Pt were then prepared by stepwise impregnation of 10 wt% CeO_2/10 wt% La_2O_3/γ-Al_2O_3 and 10 wt% CeO_2/γ-Al_2O_3 with H_2PtCl_6 solution. The catalysts were dried at 373 K and calcined at 773 K for 5 h. Unless otherwise noted, the 0.6 wt% Pt/10 wt% CeO_2/γ-Al_2O_3 catalyst is referred to as $Pt/CeO_2/Al_2O_3$ and the 0.6 wt% Pt/10 wt% CeO_2/10 wt% La_2O_3/γ-Al_2O_3 catalyst as $Pt/CeO_2/La_2O_3/Al_2O_3$.

2.2. CATALYST PRETREATMENT

The catalysts prepared by the methods outlined above are referred to as "fresh" catalysts in this report. Samples of the fresh catalysts were subjected to one of two pretreatments to study various aging effects. Thermally treated samples were subjected to dynamic aging by treatment at 1073 K for 4 h under simulated exhaust gas oscillating between lean and rich compositions at a frequency of 0.05 Hz. A detailed description of the laboratory reactor system has been reported recently [13]. The feed gas composition was 1500 vol. ppm HC (consisting of 1000 vol. ppm C_3H_6 and 500 vol. ppm C_3H_8), 1.3% CO, 0.33% H_2, 20 vol. ppm SO_2, and 974 vol. ppm NO. For the dynamic aging, the O_2 concentration was adjusted to vary the redox ratio between 0.89 (lean) and 1.16 (rich), and the N_2 concentration in the primary feed was adjusted accordingly to keep the space velocity constant. In addition to the dynamic aging, some of the samples were hydrothermally treated by aging in 10% H_2O in flowing air (200 cm^3/min) at 1223 K for 24 h.

2.3. ACTIVITY

Catalyst activity was measured using the same reactor setup as for thermal aging but without cycling the gas composition. Two types of experiments were performed, both at 60 000 h^{-1} space velocity. In the first, the catalyst temperature was increased stepwise from room temperature and the temperatures required for 50% conversion of each species (referred to as light-off temperatures) were

recorded. In the second type of experiment, conversions of CO, NO_x, and HC were measured at 823 K as a function of the molar ratio of reducing species to oxidizing species, R, varied by changing the amount of O_2 in the feed while holding the other concentrations constant ($R<1$ = excess oxidants; $R = 1$ stoichiometric; $R>1$ excess reductants).

2.4. TEMPERATURE-PROGRAMMED REDUCTION

TPR experiments were carried out on an Altamira temperature programmed system. The details of the TPR apparatus have been reported elsewhere [14]. Oxidizing pretreatments were carried out in the TPR cell in a 40 cm^3/min flow of 10% O_2 in He at 823 K for 50 min. The samples were cooled in O_2 to 277 K before the start of the temperature programmed reduction. The samples were heated in 9% H_2 in Ar to 873 K at a rate of 30 K/min and the H_2 consumption was monitored with a thermal conductivity detector.

2.5. OXYGEN STORAGE CAPACITY

The oxygen storage capacity measurements were conducted using a 3.62 cm^3 sample of the fresh and thermally aged catalysts. A thermocouple imbedded into the monolithic sample was used to monitor the temperature, while a network of solenoid valves enabled the injection of alternating pulses of carbon monoxide (1% in helium) and oxygen (0.5% in helium) at an overall flow rate of 3000 cm^3/min. Switching between gases was performed simultaneously at a frequency of 0.016 Hz, and gas sampling was accomplished through a sapphire leak valve into a quadrupole mass spectrometer using one stage of differential pumping. Oxygen storage capacity was computed from the rate of carbon monoxide removal immediately following the transition from oxygen to carbon monoxide with the sample at a temperature of 873 K.

2.6. NOBLE-METAL SURFACE AREA

A CO–H_2 titration method (i.e. methanation) [15] was used to determine Pt surface area on the $Pt/CeO_2/Al_2O_3$ and $Pt/CeO_2/La_2O_3/Al_2O_3$ catalysts. A small amount (approximately 0.1 g) of each sample was ground and packed in a glass U-tube in a "sandwich" of quartz wool. Each sample was oxidized in flowing O_2 (40 cm^3/min) for 30 min at 673 K and then reduced at 673 K in flowing H_2 (40 cm^3/min) for 30 min. After cooling the sample to room temperature in flowing H_2, two CO pulses of 2 cm^3 each were introduced to the sample with H_2 as a carrier gas. The sample was purged with H_2 for 10 min. The reactor tube was then sealed by closing three-way valves to trap the H_2 and the adsorbed CO. The sample was heated at 673 K for 30–45 min to hydrogenate the adsorbed CO. The amount of CH_4 formed after the reaction was measured by a flame ionization detector on a Varian Star 3400 gas chromatograph.

2.7. X-RAY DIFFRACTION (XRD)

XRD measurements were performed on the fresh and hydrothermally aged $Pt/CeO_2/Al_2O_3$ and $Pt/CeO_2/La_2O_3/Al_2O_3$ samples in order to determine the phases and Pt and CeO_2 particle sizes. XRD patterns were recorded on a Philips X-ray generator with a Debye-Scherrer camera. Cu Kα X-rays ($\lambda = 1.5418$ Å) were used as the X-ray source. The XRD apparatus used to analyze the samples has been described in detail previously [14].

3. Results

3.1. ACTIVITY

Light-off temperatures for fresh and thermally aged samples of both catalysts were found to be just below 773 K. This is relatively high compared to a fully formulated TWC which usually contains Rh in addition to either Pt or Pd, but is not unexpected for such a Pt-only catalyst. The R curves generated at a temperature of 823 K from the fresh catalysts are shown in figs. 1 and 2. The main differences are higher NO_x and CO conversions and lower HC conversion for the $Pt/CeO_2/$

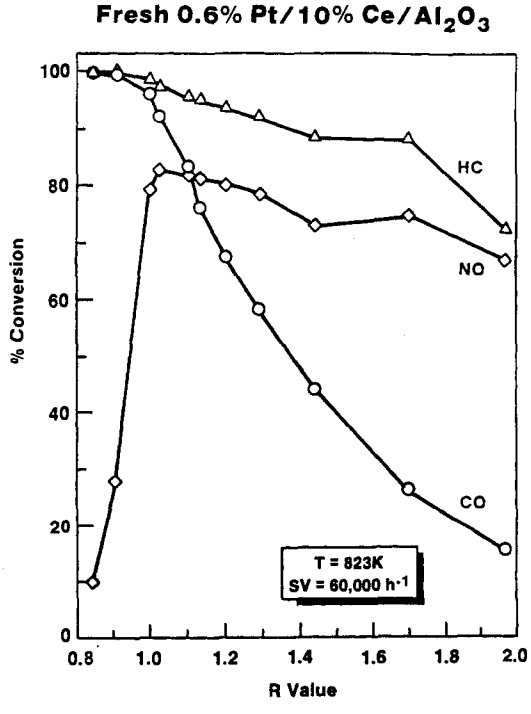

Fig. 1. Conversion efficiency of the fresh $Pt/CeO_2/Al_2O_3$ catalyst as a function of R, the molar ratio of reducing to oxidizing species in the feed gas.

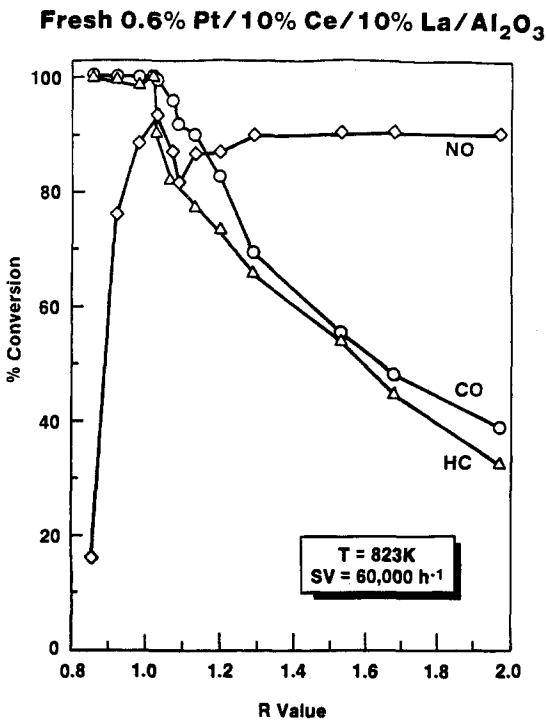

Fig. 2. Conversion efficiency of the fresh $Pt/CeO_2/La_2O_3/Al_2O_3$ catalyst as a function of R, the molar ratio of reducing to oxidizing species in the feed gas.

La_2O_3/Al_2O_3 catalyst. In addition, for the $Pt/CeO_2/Al_2O_3$ catalyst, the overall conversion of CO and HC on the rich side exceeds somewhat the O_2 and NO available, implying that water–gas shift or steam reforming reactions may be more important for this catalyst.

3.2. TEMPERATURE-PROGRAMMED REDUCTION

The reduction profiles for the $Pt/CeO_2/Al_2O_3$ and $Pt/CeO_2/La_2O_3/Al_2O_3$ catalysts after various thermal treatments are presented in figs. 3 and 4, respectively. Table 1 summarizes the H_2 consumed during reduction of these catalysts, obtained by integrating the area under the TPR traces, and compares it to the theoretical H_2 consumption.

The following trends were observed after either thermal aging in the reactor or hydrothermal aging of the fresh $Pt/CeO_2/Al_2O_3$ catalyst: (1) the broad low temperature peak (below 450 K) and the sharp peak at 515 K decreased sharply after thermal aging; these peaks were absent in the hydrothermally aged sample, (2) the broad peak around 740 K increased in size and shifted to lower temperature after thermal aging; it was absent in the hydrothermally aged sample, (3) the broad, high temperature peak extending from 800 to about 1150 K increased sharply in magni-

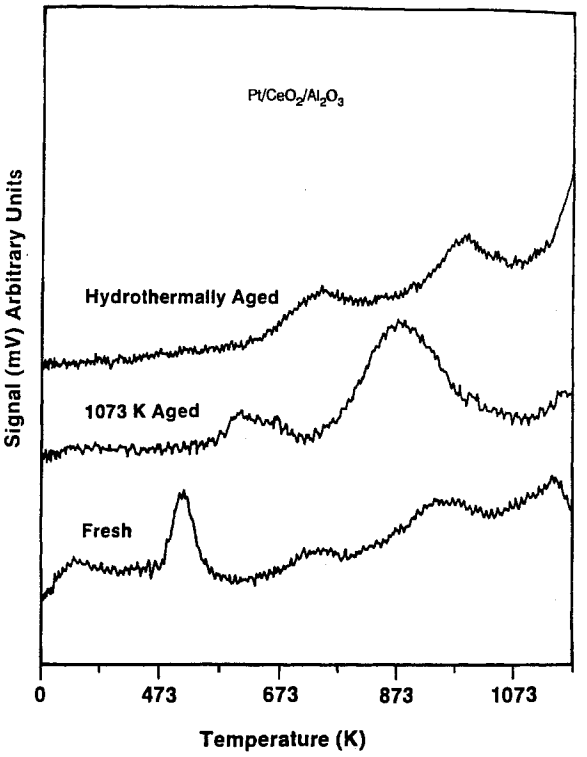

Fig. 3. TPR spectra of the $Pt/CeO_2/Al_2O_3$ catalyst after various treatments.

tude and shifted to lower temperature after thermal aging; the peak intensity decreased sharply and the maximum shifted further down to lower temperature and a new broad peak appeared at 1000 K after hydrothermal aging. Pretreatments of the $Pt/CeO_2/La_2O_3/Al_2O_3$ catalyst produced similar trends to those observed with the $Pt/CeO_2/Al_2O_3$ catalyst.

The total amount of H_2 consumed during the reduction of the fresh $Pt/CeO_2/Al_2O_3$ catalyst decreased sharply from 260 to 111 μmol/g (31.5% of the theoretical H_2 consumption) upon thermal aging. Hydrothermal aging of this catalyst proved to be harsh also, the total H_2 consumption decreasing to 131 μmol/g (37% of the theoretical H_2 consumption). In the case of the $Pt/CeO_2/La_2O_3/Al_2O_3$ catalyst, the total amount of H_2 consumed decreased from 260 μmol/g for the fresh catalyst to 194 μmol/g (55% of the theoretical H_2 consumption) for the thermally aged catalyst. The $Pt/CeO_2/La_2O_3/Al_2O_3$ catalyst thus retains more reducible oxides than the $Pt/CeO_2/Al_2O_3$ catalyst (55% of the theoretical H_2 consumption in the $Pt/CeO_2/La_2O_3/Al_2O_3$ catalyst as compared to only 31.5% in the $Pt/CeO_2/Al_2O_3$ catalyst) after thermal aging. After hydrothermal aging, however, the total amount of H_2 consumption again decreased to 131 μmol/g (37% of the theoretical H_2 consumption), identical to the decrease observed for the $Pt/CeO_2/Al_2O_3$ catalyst.

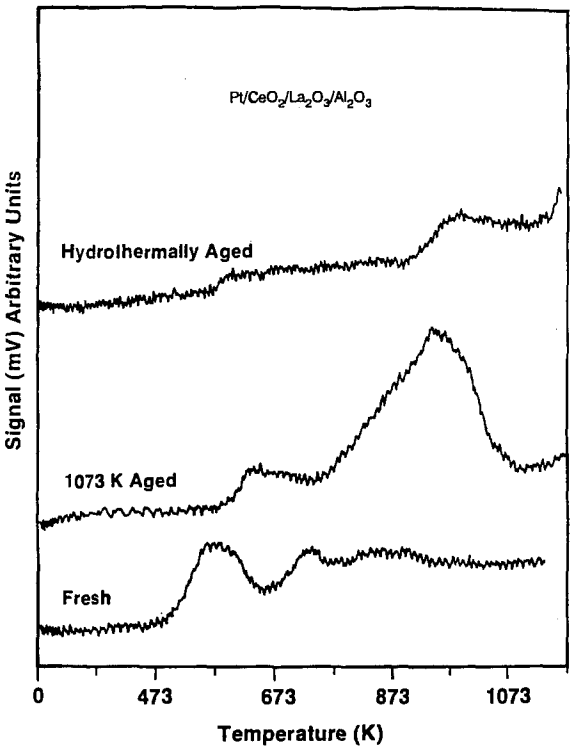

Fig. 4. TPR spectra of the $Pt/CeO_2/La_2O_3/Al_2O_3$ catalyst after various treatments.

Table 1

Sample	H_2 consumption [a] (μmol/g)	OSC [b] (μmol-O/g s)	Dispersion (%)	XRD particle size (nm)	
				Pt	CeO_2
fresh					
$Pt/CeO_2/Al_2O_3$	260	4.4	20.7	<7	8 ± 2
$Pt/CeO_2/La_2O_3/Al_2O_3$	260	9.1	24.9	<7	4 ± 2
thermally aged					
$Pt/CeO_2/Al_2O_3$	111	2.4	0.5	–	–
$Pt/CeO_2/La_2O_3/Al_2O_3$	194	5.7	4.5	–	–
hydrothermally aged					
$Pt/CeO_2/Al_2O_3$	131	–	0.65	160 ± 30	20 ± 2
$Pt/CeO_2/La_2O_3/Al_2O_3$	131	–	1.35	100 ± 30	13 ± 2

[a] Theoretical H_2 consumption is 352 μmol/g for all samples, assuming $PtO_2 \rightarrow Pt$ and $CeO_2 \rightarrow Ce_2O_3$.

[b] OSC: oxygen storage capacity.

3.3. OXYGEN STORAGE CAPACITY

Oxygen storage capacities are listed in table 1, where it can be seen that the $Pt/CeO_2/La_2O_3/Al_2O_3$ catalyst has about twice the capacity of the $Pt/CeO_2/Al_2O_3$ catalyst, both in the fresh and thermally aged states.

3.4. NOBLE-METAL SURFACE AREA

Dispersion measurements for teach sample are presented in table 1. The dispersion measurements were carried out after the pretreatments described in the experimental section. The estimated noble metal dispersions are based on the assumed ratio of $Pt_{surface\,atoms} : CO_{adsorbed} : CH_{4\,formed} = 1$. Previous studies [15] have shown that the assumed ratio of one methane molecule formed per CO molecule adsorbed is accurate.

The percentage dispersion was higher for the fresh $Pt/CeO_2/La_2O_3/Al_2O_3$ catalyst than for the fresh $Pt/CeO_2/Al_2O_3$ catalyst (24.9 and 20.7%, respectively). In all cases, the percentage dispersion dropped dramatically after aging. However, the samples with La^{3+} yielded higher Pt dispersions than the samples without La^{3+} (4.5% versus 0.5% after thermal aging and 1.35% versus 0.65% after hydrothermal aging).

3.5. X-RAY DIFFRACTION

Diffraction patterns from both fresh and hydrothermally aged samples of the two catalysts are shown in figs. 5 and 6, where differences in phase composition and Pt and CeO_2 particle size are apparent. In particular, α-Al_2O_3 is present in the $Pt/CeO_2/Al_2O_3$ sample while $LaAlO_3$ is present in the $Pt/CeO_2/La_2O_3/Al_2O_3$ sample after hydrothermal aging, and the Pt and CeO_2 particles are always smaller in the sample containing La^{3+}. Estimates of the latter, derived from line broadening, are listed in table 1.

4. Discussion

As the noble-metal surface area and XRD measurements show, the addition of La^{3+} to the $Pt/CeO_2/Al_2O_3$ catalyst has the effect of increasing both Pt and CeO_2 dispersions. A similar effect of La^{3+} on Rh dispersion, qualitatively like that of Ce^{4+}, has been observed before [16,17] and has also been reported for Pt/γ-Al_2O_3 [3]. In view of the higher dispersions, it is thus reasonable that the oxygen storage capacity should also be higher in the $Pt/CeO_2/La_2O_3/Al_2O_3$ catalyst, as observed. From the standpoint of activity, the addition of La^{3+} to the $Pt/CeO_2/Al_2O_3$ catalyst affects primarily rich-side HC conversion. A reduction in possible steam reforming activity due to higher Pt dispersion in the catalyst containing La^{3+} would

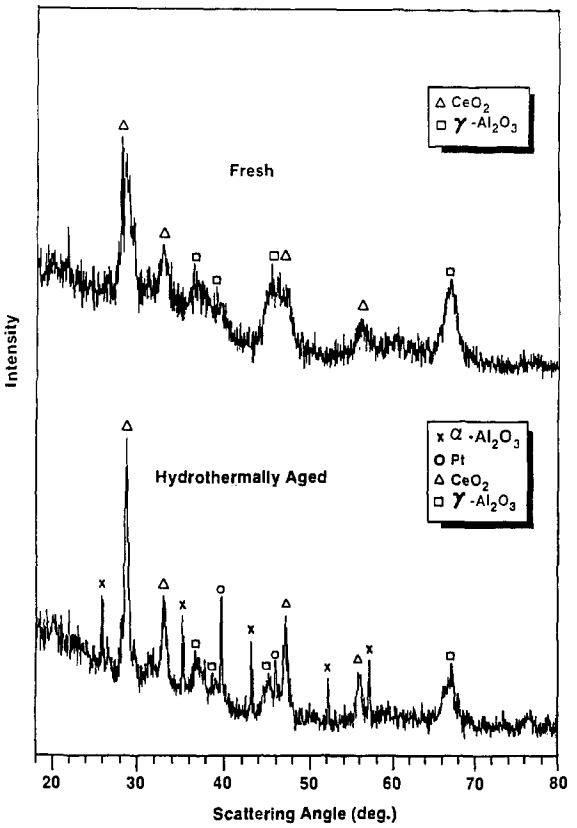

Fig. 5. Diffraction patterns for the fresh (top panel) and hydrothermally aged (bottom panel) $Pt/CeO_2/Al_2O_3$ catalyst.

be consistent with this observation if specific activity for steam reforming increases with increasing particle size. This behavior has been observed for reaction of *n*-heptane with steam over $Rh/\gamma\text{-}Al_2O_3$ [18].

Similar effects of La^{3+} are also seen after the aging treatments. Activity measurements from thermally aged samples showed the same difference in rich-side HC conversion between the two catalysts as seen in the fresh state. The promotional effect of La^{3+} on Pt and CeO_2 dispersions in these catalysts was also maintained, as shown from both the noble-metal surface area measurements following each pretreatment and the XRD measurements following the hydrothermal treatment. Additional effects beyond a simple promotion of Pt and CeO_2 dispersions are also evident. Although the TPR results indicate that the presence of La^{3+} had no effect on the amount of reducible oxides in the fresh state, the retention of a greater amount of reducibles on the surface after thermal aging suggests that La^{3+} may have blocked, to some extent, the interaction of CeO_2 with Al_2O_3 which leads to the stabilization of Ce^{3+} [19]. This effect disappears after hydrothermal aging, however. Finally, the XRD data of the hydrothermally aged catalysts indicates that

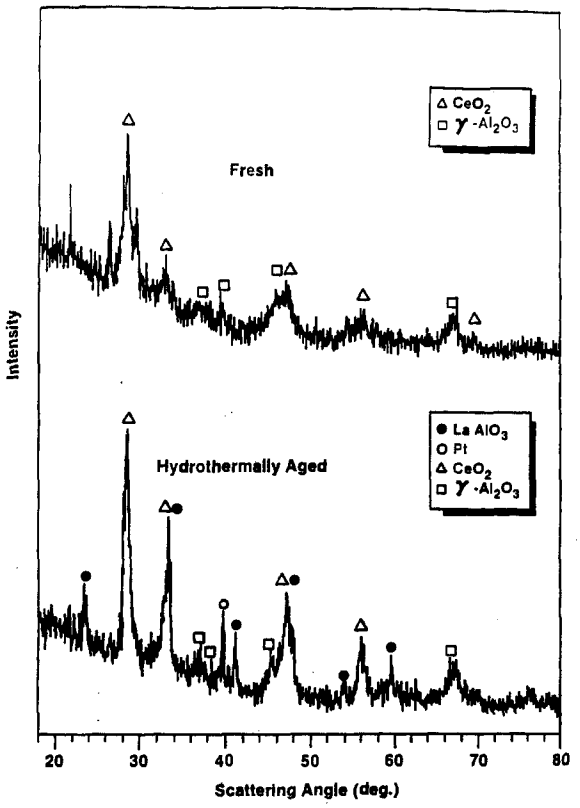

Fig. 6. Diffraction patterns for the fresh (top panel) and hydrothermally aged (bottom panel) $Pt/CeO_2/La_2O_3/Al_2O_3$ catalyst.

La^{3+} forms $LaAlO_3$ with Al_2O_3 and prevents α-Al_2O_3 formation while the alpha phase of Al_2O_3 is clearly seen in the diffraction pattern from the catalyst without La^{3+}.

In summary, this study shows that La^{3+} increases the dispersion of Pt and CeO_2 and inhibits to some extent the interaction between CeO_2 and Al_2O_3. The mechanism by which it inhibits the interaction of CeO_2 with Al_2O_3 appears to involve formation of its own compound with Al_2O_3. Higher dispersions of Pt and CeO_2 and the retention of a greater range of reducible oxides on the surface translate into an improved oxygen storage capacity.

Acknowledgement

The authors appreciate the assistance of the late C.R. Peters in providing the X-ray identification of the alumina phases and ceria and Pt particle size. We also appreciate the assistance of F.W. Kunz with the XRD data. Useful discussions were held with M. Shelef and J.S. Hepburn.

References

[1] B. Beguin, E. Garbowski and P. Primet, J. Catal. 127 (1991) 595.
[2] H. Muraki, H. Yokota and Y. Fujitani, Appl. Catal. 48 (1989) 93.
[3] V.A. Drozdov, P.G. Tsyrul'nikov, V.V. Popovskii, Y.D. Pankrat'ev, A.A. Davydov and E.M. Moroz, Kinet. Catal. 27 (1986) 721.
[4] G.W. Graham, P.J. Schmitz, R.K. Usmen and R.W. McCabe, Catal. Lett. 17 (1993) 175.
[5] J.Z. Shyu, W.H. Weber and H.S. Gandhi, J. Phys. Chem. 92 (1988) 4964.
[6] E.C. Su and W.G. Rothschild, J. Catal. 99 (1986) 506.
[7] H.C. Yao and Y.F. Yu Yao, J. Catal. 86 (1984) 254.
[8] H.S. Gandhi, A.G. Piken, M. Shelef and R.G. Delosh, SAE 760201 (1976) 55.
[9] Y.F. Yu Yao and J.T. Kummer, J. Catal. 106 (1987) 307.
[10] M. Ozawa and M. Kimura, J. Mater. Sci. Lett. 9 (1990) 291.
[11] J.C. Schlatter and P.J. Mitchell, Ind. Eng. Chem. Prod. Res. Dev. 19 (1980) 288.
[12] G. Kim, Ind. Eng. Chem. Prod. Res. Dev. 21 (1982) 267.
[13] R.K. Usmen, S. Subramanian, R.W. McCabe and R.J. Kudla, SAE (1993) 933036.
[14] R.K. Usmen, R.W. McCabe, G.W. Graham, W.H. Weber, C.R. Peters and H.S. Gandhi, SAE (1992) 922336.
[15] R.K. Usmen, R.W. McCabe and M. Shelef, in: *Proc. Third Congress on Automotive Pollution Control*, Brussels, April 1994, to be published.
[16] R. Alvero, A. Bernal, I. Carrisona and J.A. Odriozola, Inorg. Chim. Acta 140 (1987) 45.
[17] R.K. Usmen, R.W. McCabe, L.P. Haack, G.W. Graham, J. Hepburn and W.H. Watkins, J. Catal. 134 (1992) 702.
[18] E. Kikuchi, K. Ito, T. Ino and Y. Morita, J. Catal. 46 (1977) 382.
[19] M. Shelef, private communication (1990).